Wood Diaphragm Deflections. II: Implementing a Unified Approach for Current CLT and WSP Practice

John Lawson, S.E., M.ASCE[1]; Scott Breneman, Ph.D., M.ASCE[2]; and Marco Lo Ricco, Ph.D., M.ASCE[3]

Abstract: Horizontal wood diaphragm systems, whether decked with conventional or mass timber panels, transfer wind and seismic loads to vertical elements of the lateral force-resisting system, in flexible, rigid, or semirigid ways. Characterizing and calculating the resulting diaphragm deflections will help determine the distribution of forces to critically loaded components and a significant portion of lateral building translations and rotations. Deflection equations for sheathed wood structural panel (WSP) diaphragms are well established in US design standards in a four-term expression that models flexural, shear, and fastener-slip deformations, but similar equations for cross-laminated timber (CLT) diaphragms have yet to unfold, despite growing industry consensus that CLT panels make efficient slabs and decks. Building code standards require CLT diaphragm deflections be computed using the principles of engineering mechanics. The current three-term and four-term deflection equations for WSP diaphragms are based on various assumptions that are often outpaced by current design practices. This is the second of two companion papers, in which the first paper provides the full generalized derivation of the current four-term WSP diaphragm deflection expression with a mechanics-based expansion to unify both potential WSP and CLT applications. This second paper builds on the first paper by expanding the generalized equation with implementation insights unique to WSP and CLT diaphragms. The various challenges of calculating diaphragm deflections associated with the current design practices are discussed with suggestions to assist in implementation. **DOI: 10.1061/JAEIED.AEENG-1574.** *© 2023 American Society of Civil Engineers.*

Practical Applications: In general, the computation of diaphragm deflections has become increasingly important ever since equations were first developed for WSP systems around 70 years ago. Deflections are routinely computed to evaluate building separations, property line setbacks, P-delta instability, and evaluation of nonstructural damage from interstory drift. Additionally, appropriate engineering modeling requires accurate diaphragm stiffness values to characterize diaphragms as rigid, semirigid, or flexible. The mechanics-based equations in this paper are presented in a form that will be useful to today's practitioners to produce more rational building designs.

Introduction

Engineered wood building diaphragms using plywood structural panels or oriented strand board (OSB) are common in the United States (US) and globally. Collectively referred to as wood structural panels (WSP), these panels typically measure 1,220 × 2,440 mm (4 × 8 ft) of rectilinear area and up to 28.5 mm (1⅛ in.) of thickness in nominal unitized dimensions. Given the importance of horizontal wood diaphragms in resisting a variety of loads (such as earth, wind, and seismic) acting transversely to wall planes (Cobeen et al. 2014), design procedures for WSP diaphragms are well established in the US building code standards. Deflection equations for WSP diaphragms in the latest edition of the American Wood Council's *Special Design Provisions for Wind and Seismic* (SDPWS) (AWC 2021) were derived using the principles of engineering mechanics, but past corrections and simplifications have obscured the origins over time. In a companion paper by Lawson et al. (2023), the complete corrected derivation is re-established and generalized to develop appropriate user-friendly equations that may apply to a variety of panel and fastener diaphragm assemblies encountered in the current design practices.

Over the last decade, cross-laminated timber (CLT) has emerged as a new dimensionally stable, massive composite timber product, comparable with precast concrete panels in size but typically weighing eighty percent less (Gagnon et al. 2013). CLT buildings have garnered international attention for rapid erection of tall wood structures with smaller carbon footprints. CLT originated in Europe and production has spread globally. In cities throughout the United States, including seismically active regions of the West and high-wind regions of the coastal South and East, a majority of engineers have stated that they are likely to adopt CLT construction in a future project if given the choice (Laguarda-Mallo and Espinoza 2018). Contemporary tall wood construction has produced a variety of building archetypes, including predominantly wood and hybrid structural schemes (Foster et al. 2016). The most common use of CLT in building construction is in the form of floor and roof decking, where direct use of the CLT deck as a diaphragm system is economically attractive. For CLT diaphragms, SDPWS states that deflections shall be determined using the principles of engineering mechanics (AWC 2021), yet no deflection equations have been directly provided. The motivation to develop similarly established diaphragm deflection models and ways to implement them for CLT panel diaphragms, therefore, leads us to present a mechanics-based approach to guide practitioners and researchers.

[1]Professor, Dept. of Architectural Engineering, California Polytechnic State Univ., San Luis Obispo, CA 93407 (corresponding author). ORCID: https://orcid.org/0000-0002-3237-5929. Email: jwlawson@calpoly.edu

[2]Senior Technical Director—Mass Timber Program Manager, WoodWorks—Wood Products Council, PO Box D, Deer Park, WA 99006. ORCID: https://orcid.org/0000-0003-1189-1374. Email: scott.breneman@woodworks.org

[3]Research General Engineer, USDA Forest Service, Forest Products Laboratory, One Gifford Pinchot Drive, Madison, WI 53726. ORCID: https://orcid.org/0000-0001-9940-1602. Email: marco.loricco@usda.gov

Note. This manuscript was submitted on October 12, 2022; approved on March 27, 2023; published online on May 29, 2023. Discussion period open until October 29, 2023; separate discussions must be submitted for individual papers. This paper is part of the ***Journal of Architectural Engineering***, © ASCE, ISSN 1076-0431.

Diaphragm deflections determine whether a diaphragm may be idealized as flexible (ASCE/SEI 7-22, ASCE 2022; AWC 2021) or rigid (AWC 2021; ICC 2021) or what stiffness factor to use in a semirigid approach. Deformation compatibility, torsional irregularities, and building separations are additionally influenced by this computation. The relative stiffness of the diaphragm and vertical elements, furthermore, calibrates the results of numerical earthquake response time–history analyses used for making a detailed evaluation of structures. An overestimation of diaphragm deflection may lead to a conservative sizing of seismic joints but also to an underestimation of period-based seismic forces caused by diaphragm stiffness (Lawson 2019). Because of the trend of using period-based seismic forces in diaphragms (FEMA 2021; ASCE/SEI 41-17, ASCE 2017), the Building Seismic Safety Council identified the computation of period-based diaphragm stiffness as an important current research need (BSSC 2021). This paper adapts the generalized diaphragm deflection equation presented in a companion paper (Lawson et al. 2023) to common WSP and CLT construction assemblies to keep pace with the current construction detailing practices with computations based on the established principles of engineering mechanics.

Standard Deflection Equations of Diaphragms Sheathed with Wood Structural Panels

The current US practice of calculating wood-sheathed diaphragm deflections is based on modified forms of Eq. (1), a four-term equation published in the SDPWS Commentary (AWC 2021). For definitions of the parameters appearing in the equations and figures, throughout this paper, see *Notation*.

$$\delta_{\mathrm{dia,US}} = \frac{5vL^3}{8EAW} + \frac{vL}{4G_v t_v} + 0.188 L e_n + \frac{\sum(x\Delta_c)}{2W} \tag{1}$$

Eq. (1), developed for customary units used by US designers, includes implicit unit conversions in the first and third terms. This equation was developed specifically for uniformly loaded simple span diaphragms, to quantify the four sources of deflection schematically illustrated in Fig. 1. In respective order of the terms, Eq. (1) estimates the contributions from flexural deformation, shear-induced panel deformation, diaphragm deformation associated with the nail slip, and the effects of the flexural chord connection slip. The four terms of Eq. (1) can be written as follows:

$$\delta_{\mathrm{dia}} = \delta_{\mathrm{flex}} + \delta_{\mathrm{shear}} + \delta_{\mathrm{slip}} + \delta_{\mathrm{chord}} \tag{2}$$

Similar expressions are found in the Canadian Standard *Engineering Design in Wood* (CSA 2019) and the New Zealand *Timber Structures Standard* commentary clauses (NZS 1993).

Because of common WSP construction detailing and practices, Eq. (1) and other standard variations assume the following:

- Panels measure 1.22 m (4 ft) by 2.44 m (8 ft) in size, as viewed in the plan,
- Shear fasteners used on all edges of all panels (e.g., nails) are the same type and size,
- Shear fastener spacing is equal around all edges of all panels,
- Detailing follows the conventions of blocked diaphragms, and
- Axial chord forces act at the edges of the diaphragm.

Since the 2001 edition of SDPWS was released, a three-term expression that combines the effects of panel shear deformation and fastener slip into one term has been the standardized deflection equation for WSP diaphragms.

$$\delta_{\mathrm{dia,US}} = \frac{5vL^3}{8EAW} + \frac{0.25vL}{1{,}000G_a} + \frac{\sum(x\Delta_c)}{2W} \tag{3}$$

SDPWS presents the four-term Eq. (1) and the approximation used to reduce it to the three-term form in the Commentary.

Eqs. (1) and (3) present terms published in US design standards, which use US customary units for each variable as a shortcut for common practice. For example, L is in feet, and the deflection, $\delta_{\mathrm{dia,US}}$ is in inches. This paper will use the subscript "US" to distinguish when an equation uses US customary units and implicit unit conversions. The US customary units for each variable are listed in the *Notation* section of this paper. Equations without the subscript "US" do not have implicit unit conversions and may be generally applied to any system of units.

Generalized and Expanded Deflection Equation

In Lawson et al. (2023), Eq. (1) is fully derived and expanded into Eq. (4) for generalized use with any standard system of measure and with potential application to a broader variety of WSP and CLT diaphragms.

$$\delta_{\mathrm{dia}} = \frac{5vL^3}{96EAW} + \frac{vL}{4G_v t_v} + \frac{L}{4}\left(\frac{n_{\parallel} e_{f\parallel}}{P_{\perp}} + \frac{n_{\perp} e_{f\perp}}{P_{\parallel}}\right) + \frac{\sum(x\Delta_c)}{2W} \tag{4}$$

Eqs. (1) and (4) assume a uniformly loaded, simple span wood panel diaphragm with diaphragm chords located at the diaphragm edges. An appendix in conjunction with the derivations in Lawson et al. (2023) provides the necessary tools for practitioners to evaluate different configurations and loadings.

The primary improvements that Eq. (4) has over Eq. (1) are observed in the third term, which represents the effect of the fastener slip. In the third term of Eq. (1), a single value of nail slip e_n is expressed, limiting its theoretical usefulness to panels with only one type of fastener and one spacing along the perimeter edges of each panel. However, Eq. (4) can track the fastener slip, e_f, on the panel edges parallel and perpendicular to the diaphragm load direction independently, thus accounting for two different types of fasteners and fastener spacings on the panel edges. The computation of $e_{f\parallel}$ and $e_{f\perp}$ is based on the static equilibrium model as derived in Lawson et al. (2023) and illustrated in Fig. 2. In Fig. 2, the nail fasteners are equally spaced around all panel edges, and therefore, the shear per nail parallel to the adjacent panel edge, V_n, is assumed to have equal magnitude for all nails. Differences in fastener spacings will create differences in fastener shears.

The ability to consider different fastener spacings at the panel edges is useful in current practice because many of the specified nailing patterns in the blocked diaphragms of SDPWS Tables 4.2A and 4.2B have different nail spacings in the direction parallel to the load compared with the direction perpendicular to the load. When using a staggered panel layup, SDPWS Tables 4.2A and 4.2B allow a wider spacing on the edges which are not continuous across the diaphragm in the direction of the applied load. For example, Fig. 3 shows a possible nailing pattern with three different nail spacings along the perimeter of panels specified as (1) the diaphragm boundaries, (2) continuous panel edges, and (3) staggered panel edges. The variety of nailing patterns may increase, if the designer looks to economize fasteners, based on varying shear forces. Under distributed loads, the shear stresses vary along the length of the diaphragm, and designers may opt to vary the fastener spacing along the length of the diaphragm rather than provide constant fastener spacings. It is common for WSP diaphragms in big-box buildings to economize the number of fasteners and have varied nail

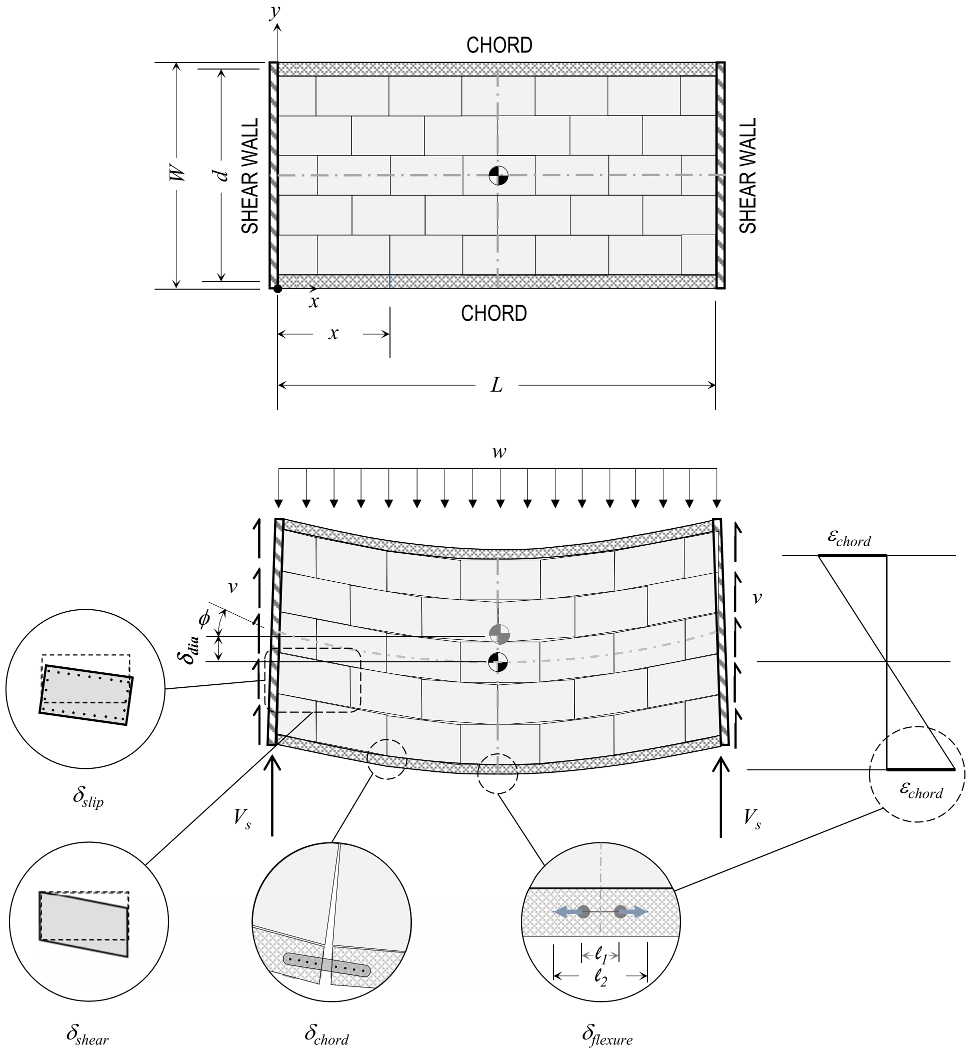

Fig. 1. Deflection parameters of a simple span diaphragm.

spacings throughout (Lawson 2012; SEAOC 2019), and this building archetype often exhibits significant deflections of the diaphragm (FEMA 2021; Lawson and Koliou 2020). The ability to independently address both different fastener types and spacings on the different panel edges is also useful for CLT. For example, it is common practice to use plywood splines with nails or short screws between panels at the long panel edges and long screws through the panels to the framing below at the short panel edges (Line et al. 2022a, b).

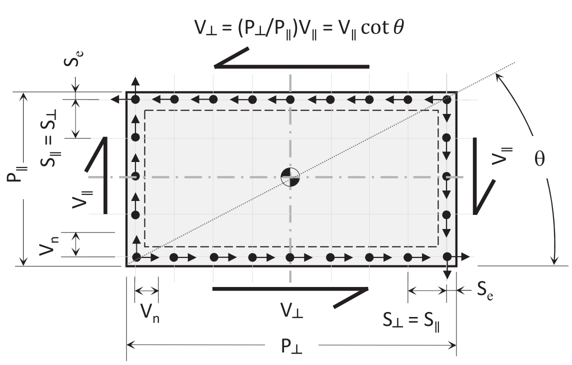

Fig. 2. Panel dimensions, fastener spacings, and shear forces.

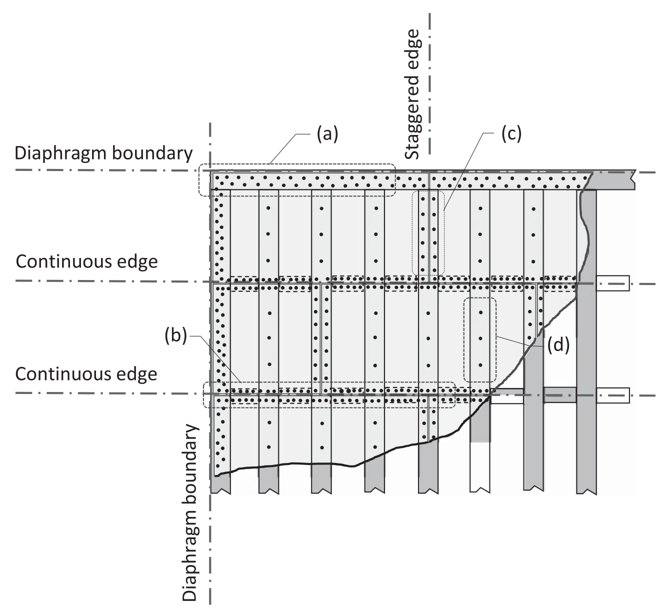

Fig. 3. Partial plan view of a blocked diaphragm nailing pattern with different spacings at (a) boundaries; (b) continuous panel edges; (c) staggered edges; and (d) interior field of panels.

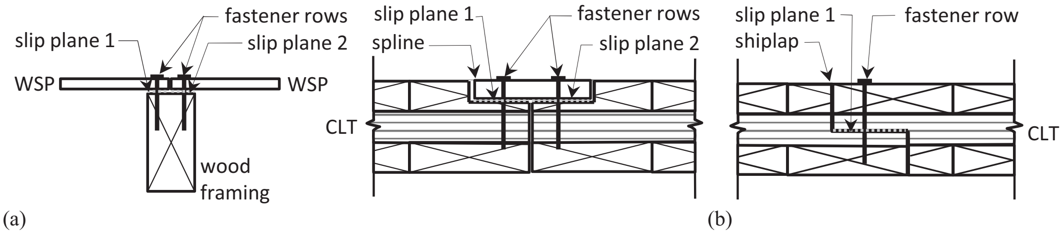

Fig. 4. Fastener-slip planes in typical panel connections of (a) WSP; and (b) CLT diaphragms.

Eq. (1) bases the computation of the nail slip e_n on a single, uniform value that assumes the same fastener spacing on along all four edges of the panel perimeters. SDPWS Table C4.2.3D provides formulae for computing e_n based on the shear per nail, V_n, where V_n is computed as the diaphragm boundary shear per unit length divided by the nail spacing. The boundary and continuous edge nailings, however, often differ from the other staggered edge nailings, per detailing requirements (AWC 2021). Because the fastener spacings along the edges parallel and perpendicular to the applied diaphragm loads are often different, determining a single fastener slip to use requires an engineering judgment or approximation. Tissell and Elliott (2004) state that if different spacings are combined on the same WSPs, the larger spacings should be used, and this is the approach that the AWC took when developing G_a in Eq. (3) (AWC 2021). When nail spacings vary, this approach will overestimate the computation of diaphragm deflections, but will unconservatively underestimate the computation of period-based seismic forces. The use of Eq. (4) helps avoid this discrepancy by explicitly using terms that vary the number and slip of fasteners along the respective panel edges.

An additional feature of Eq. (4) is its ability to address the number of slip planes, n, for shear transfer from one panel to its neighbor. In blocked WSP diaphragms, there are typically two slip planes as the load moves from the panel to the framing and then from the framing to the neighboring panel [Fig. 4(a)]. In CLT, splined connections also have two slip planes. Half-lap connections are used in some diaphragms to provide stronger and stiffer connections than achievable with spline connections. The half-lap connection creates a single slip-plane condition [Fig. 4(b)]. Several recent studies address the connection behavior of these spline and half-lap connections in CLT (Sullivan et al. 2018; Taylor et al. 2020, 2021).

Eq. (4) can also track the effects of panel dimensions that differ from the assumed 1,220 × 2,440 mm (4 × 8-ft) used in the derivation of Eq. (1). Because CLT panels do not have standardized widths and lengths comparable with WSP, Eq. (4) is more directly applicable. Nonstandard WSP sizes such as 1,220 × 3,048 mm (4 × 10-ft) or 2,440 × 2,440 mm (8 × 8-ft) jumbo panels are also used in diaphragm construction, which provides a further incentive to use the generalizations of Eq. (4).

With the value of Eq. (4) now evident, this paper will adapt the model to a variety of common WSP and CLT practices.

Fastener Slip Refinements for WSP Diaphragms

It is useful to adapt the general-use Eq. (4) to address the issue of the common occurrence of different nail spacings on the panel edges parallel and perpendicular to the diaphragm load direction. If different fastener spacings $S_\parallel$ and $S_\perp$ are regular and uniform along each respective edge and parameter b is defined as the ratio of $S_\perp/S_\parallel$, then the fastener slip along the panel edges perpendicular to the diaphragm load, $e_{f\perp}$, in terms of $e_{f\parallel}$, is as written in Eq. (5) for linear behavior:

$$e_{f\perp} = \frac{S_\perp}{S_\parallel} e_{f\parallel} = b e_{f\parallel} \tag{5}$$

Substituting Eq. (5) for $e_{f\perp}$ into the third term of Eq. (4) yields a simplified form:

$$\delta_{\text{slip}} = \frac{e_{f\parallel} L}{4}\left(\frac{n_\parallel}{P_\perp} + \frac{b n_\perp}{P_\parallel}\right) \tag{6}$$

For WSP diaphragms, current practice always uses two slip planes along each adjoining edge, therefore

$$\delta_{\text{slip}} = \frac{e_{f\parallel} L}{2}\left(\frac{1}{P_\perp} + \frac{b}{P_\parallel}\right) \tag{7}$$

Eqs. (4) and (7) rely on an accurate assessment of the fastener slip e_f. The fastener slip can be computed from the shear per fastener V_f divided by the fastener stiffness γ, as expressed by

$$e_f = \frac{V_f}{\gamma} \tag{8}$$

Tests of WSP diaphragm systems have historically exhibited nonlinear lateral load-slip fastener bearing relationships. SDPWS Table C4.2.3D (AWC 2021) provides load-slip formulae with exponents to characterize the nonlinear behavior of nails up to an allowable load. Plate I plotted by Countryman (1952) and subsequent studies provide the empirical data that APA engineers later used to statistically fit and determine these relationships (Skaggs and Martin 2004). Fig. 5(b) plots the load-slip equations for three sizes of common, smooth-shank nails into dry lumber and laterally loaded by WSP side members that meet the requirements of a Structural I sheathing classification. Because the magnitude of lateral shear on fasteners within a uniformly loaded diaphragm typically varies, calculating the fastener slip e_f in Eq. (8) based on a single value of linear shear stiffness, γ, introduces some error due to the actual nonlinear fastener behavior that contributes to diaphragm deflection. Fasteners near diaphragm supports, where unit shears are typically the highest, slip further along the load-displacement curve than fasteners near low-shear regions, such as the midspan of a uniformly loaded simple span diaphragm. The slopes of the shear–slip curve in each fastener loading condition, therefore, give a different stiffness value. For common nails, SDPWS Table C4.2.3D estimates this nonlinear behavior with exponential equations for nail slip e_n (inches) based on the general format of Eq. (9).

$$e_n = (V_n/\gamma)^a \tag{9}$$

Eq. (9) may be customized to estimate slip e_f more generally for dowel-type fasteners if the parameters are substantiated with test data. If the load slip is to be restricted to the near-linear elastic range, then the exponential term, a, may equal 1. If operating beyond the proportional limit and still within safe working capacity of the joint, a may be determined as a value greater than 1, by fitting the exponential function to the test data of the nonlinear load slip.

In typical WSP diaphragms, crews install a uniform fastener size and type but often vary the fastener spacing to comply with the engineering details. Regardless of spacing, identical fasteners that are consistently driven into the same materials are assumed to follow the same lateral load–displacement curve, and therefore, a and γ are the same for $e_{f\parallel}$ and $e_{f\perp}$. However, the shear per fastener along the edges parallel and perpendicular to the diaphragm loaded direction ($V_{f\parallel}$ and $V_{f\perp}$) will vary depending on the panel dimensions $P_\parallel$ and $P_\perp$ and fastener spacings $S_\parallel$ and $S_\perp$, respectively. More specifically, Eq. (10) computes the shear per fastener along the panel edges that are parallel to the diaphragm load direction.

$$V_{f\parallel} = \frac{V}{P_\parallel / S_\parallel} = \frac{VS_\parallel}{P_\parallel} \tag{10}$$

Substituting Eq. (10) into Eq. (9) for general fasteners:

$$e_{f\parallel} = (V_{f\parallel}/\gamma)^a = \left(\frac{VS_\parallel}{\gamma P_\parallel}\right)^a \tag{11}$$

Similarly, the fastener slip along the edges perpendicular to the loaded direction is

$$e_{f\perp} = (V_{f\perp}/\gamma)^a \tag{12}$$

The load per fastener $V_{f\perp}$ is the shear along the perpendicular edge from Fig. 2 divided by the number of fasteners:

$$V_{f\perp} = \frac{\frac{P_\perp}{P_\parallel} V_\parallel}{P_\perp / S_\perp} = V_\parallel \frac{S_\perp}{P_\parallel} \tag{13}$$

Instead of the actual spacings, it will prove simpler to consider the ratio of spacings b equal to $S_\perp / S_\parallel$. Rearranging and substituting $bS_\parallel$ for $S_\perp$ in Eq. (13), the following is obtained:

$$V_{f\perp} = b\left(\frac{V_\parallel S_\parallel}{P_\parallel}\right) \tag{14}$$

Integrating Eq. (10) into Eq. (14) will yield

$$V_{f\perp} = bV_{f\parallel} \tag{15}$$

Integrating Eq. (15) into Eq. (9) will yield

$$e_{f\perp} = (bV_{f\parallel}/\gamma)^a = b^a (V_{f\parallel}/\gamma)^a = b^a e_{f\parallel} \tag{16}$$

Integrating Eq. (16) into Eq. (7) and simplifying will yield Eq. (17) for a uniformly distributed loaded diaphragm constructed of any rectangular wood panel size and orientation with consistent fastener types but at potentially different spacings, along the parallel versus perpendicular edges relative to the diaphragm load direction.

$$\delta_{\text{slip}} = \frac{e_{f\parallel} L}{2}\left(\frac{1}{P_\perp} + \frac{b^a}{P_\parallel}\right) \tag{17}$$

Eq. (17) provides researchers and practitioners with a rational approach to evaluate blocked WSP diaphragms commonly implemented today. Eq. (17) may apply to different nail spacings on the continuous panel edges and diaphragms with any panel sizes or orientations. The use of Eq. (17) instead of the third term of Eq. (1) will always result in a smaller diaphragm deflection nail slip contribution for all SDPWS Table 4.2A and 4.2B diaphragms with closer nail spacings along the continuous panel edges compared with the other staggered edges (Lawson 2018).

Integrating Eq. (17) into the generalized diaphragm deflection Eq. (4) yields Eq. (18), which is useful under any standard system of measure for WSP diaphragms designed under current practices with continuous edge nailing that differs from the other staggered edges.

$$\delta_{\text{dia}} = \frac{5vL^3}{96EAW} + \frac{vL}{4G_v t_v} + \frac{e_n L}{2}\left(\frac{1}{P_\perp} + \frac{b^a}{P_\parallel}\right) + \frac{\sum (x\Delta_c)}{2W} \tag{18}$$

Eq. (19) is provided for customary units used by US designers, which includes implicit unit conversions in the first term:

$$\delta_{\text{dia.US}} = \frac{5vL^3}{8EAW} + \frac{vL}{4G_v t_v} + \frac{e_n L}{2}\left(\frac{1}{P_\perp} + \frac{b^a}{P_\parallel}\right) + \frac{\sum (x\Delta_c)}{2W} \tag{19}$$

Fastener Slip Refinements for CLT Diaphragms

In contrast to WSP diaphragms, CLT diaphragms commonly have fasteners with different stiffnesses on the long versus short panel edges. The diaphragm connections along the long edge of CLT panels are frequently nailed plywood splines, while the connections along the short edge of the CLT panels are frequently screws penetrating the depth of the panel into a supporting element below. A similar simplification of the nail slip term seen in Eq. (17) is not possible. Instead, the generalized Eq. (4) is used, starting with computing the panel edge shears $V_\parallel$ and $V_\perp$ (Fig. 2) to compute fastener shears $V_{f\parallel}$ and $V_{f\perp}$ based on fastener edge spacings $S_\parallel$ and $S_\perp$ and then determining their resulting fastener slips $e_{f\parallel}$ and $e_{f\perp}$. Fastener manufacturers may provide a single fastener stiffness value at the allowable stress design or load resistance factor design capacity from which a linear relationship might be assumed. Screws attaching the CLT panels to the wood supports are typically proprietary, and the manufacturer may have useful data on their load-slip behavior to determine the fastener stiffness γ. For nails, screws, and bolt fasteners, Eurocode 5 (CEN 2004) provides a generic shear-slip model of equations that apply to service conditions, in which 40% of ultimate capacity sets a safe working limit and the fastener shear stiffness follows a linear elastic load path. The model plotted in Fig. 5(a), based on Eurocode 5 methodology dowel-type fasteners, defines stiffness, K_{service}, as the secant modulus of the load–displacement curve at the safe working limit. US standards adopt a similar model but with a 5-percent-of-diameter offset from the linearly approximated stiffness to determine the yield load V_y of the fastener (AWC 2015).

Application to WSP Diaphragms

A few observations on the application of the four separate equation terms to calculating the deflections of WSP diaphragms are noteworthy. The diaphragms' flexural contribution from the chord's axial deformation is directly associated with the diaphragm chord stiffness, EA. An evaluation of chord properties from perimeter beams or wood-framed top plate(s) or the horizontal reinforcing steel of concrete or masonry walls is necessary to accurately model the condition of stiffness. Additional stiffnesses from continuous crosstie framing and transverse walls have been observed (Dolan et al. 2003; Pang et al. 2014; Zapata-Kraft et al. 2022).

The shear deformation contribution term may need to be adjusted for situations where the diaphragm is comprised of different panel thicknesses or grades. In the design practice of large WSP diaphragms, engineers find it more economical to use multiple zones of unique diaphragm nailing patterns and/or panel thicknesses to accommodate the different levels of shear. Tighter nail spacings are specified near the higher-stressed diaphragm boundaries compared with the lower-stressed diaphragm interiors. The 0.188 coefficient on the nail slip contribution term of Eq. (1) is based on using the same nailing on all panel edges across the entire diaphragm.

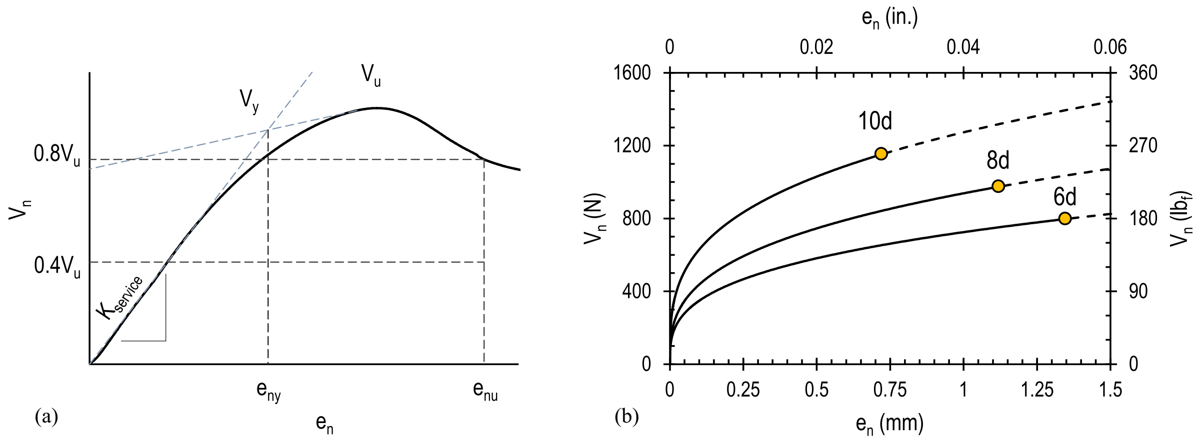

Fig. 5. Fastener models for (a) linear elastic stiffness at service loads; and (b) nonlinear slip of common nails in dry lumber.

When varying fastener spacing for achieving efficiency in large diaphragms, it is appropriate to evaluate the various fastener spacing pattern zones as individual contributions to the total fastener slip contribution (Lawson 2012; SEAOC 2019; Skaggs and Martin 2004). Combining the necessary diaphragm nailing zones from the two orthogonal design force directions results in a rectangular "bulls-eye" nailing zone pattern and is illustrated in FEMA P-1026 (FEMA 2021). Because bulls-eye nailing patterns efficiently vary spacing across two dimensions of the diaphragm plane, deflection computation methodologies that consider only the variation of spacing zones across one dimension would overestimate the overall nail-slip deflection contribution and therefore underestimate the overall diaphragm stiffness of the bulls-eye scheme.

The contributions from the chord splice slip, found in the fourth term of the deflection equation, should consider all connection deformation contributions such as oversized holes in the connecting plates or straps and load-slip deformation of the fasteners themselves. If the chords have practically no slip, such as splices made with welded steel or monolithic reinforced concrete, the chord slip term drops out of the diaphragm deflection model.

Application to CLT Diaphragms

In contemporary mass timber post-and-beam archetypes, CLT diaphragms are typically supported by a glulam timber framing that creates a couple of different connection conditions along the panel edges (Spickler et al. 2015). When beams span parallel to the edges of diaphragms, the spandrel beams may be designed and detailed to act as diaphragm chords. When no spandrel beam is provided along the diaphragm edge, CLT panels may form a continuous chord using steel strap splices that bridge the panel joints for producing tensile chord force. When the long direction of panels aligns with the chord forces of the diaphragm, as illustrated in Fig. 6(a), steel straps bridge the end joints of the panels and engage the effective width, b_{eff}, of the chord zone that can measure a maximum full width of the outermost panel or lesser width if splice connections are localized. Alternatively, CLT panels may be oriented transversely to the chord direction, as shown in Fig. 6(b), which could limit the b_{eff} dimension based on the distance from the panel end and centerline of the outermost strap. Designers are cautioned when distributing chord forces within CLT panels at the strap connections because the distribution is not necessarily

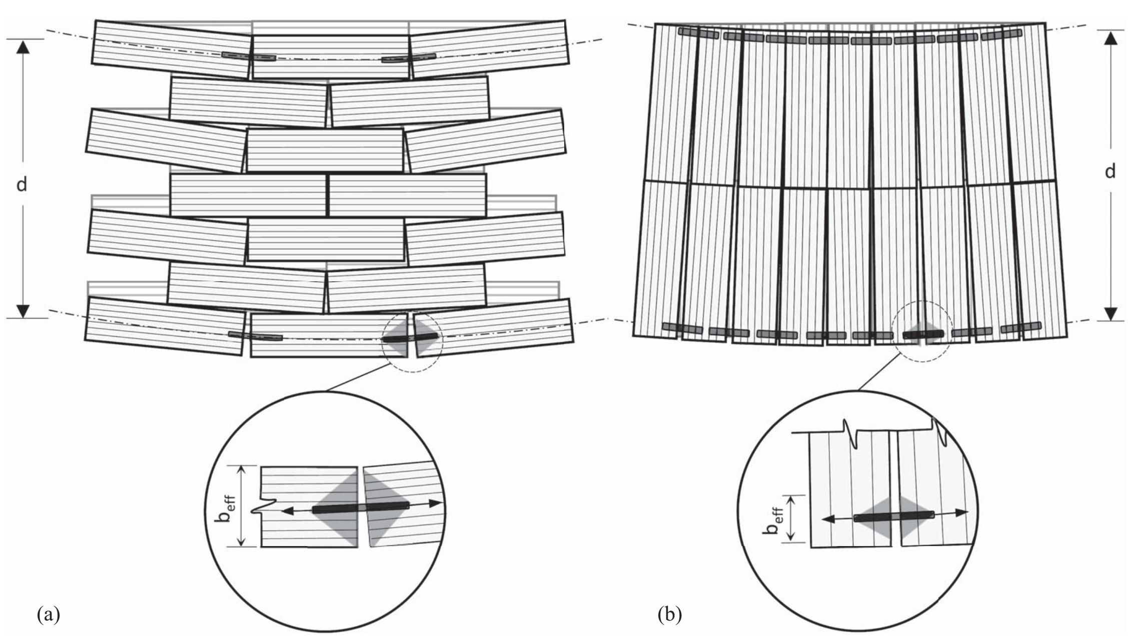

Fig. 6. CLT diaphragm chord splices: (a) end to end; and (b) side by side.

intuitive, and more research would benefit this understanding (Bhardwaj et al. 2021). An additional consideration is that the strain in each splice strap affects the stiffness of the chord system and is best addressed as contributions to the chord slip term in Eq. (4). Instead of many short strap splices as shown in Fig. 6(b), the designer may elect to simply use very long steel straps as the chord, nailed or screwed to the CLT panels along the lengths of the straps. These straps are commercially available as large coils of 12–16 m (40–55 ft) in length and up to 2.7 mm (12-gauge) thickness. With continuous straps as chords, the slip at the regularly spaced fasteners between the straps and the panels is a form of fastener slip accounted for in the fastener slip term based on the typical panel-to-panel connection perpendicular to the diaphragm load direction. With continuous chord straps, the chord slip term is used to capture any additional localized slip that may occur at strap splices or similar, if they are present in the detailing. This is similar to how the chord slip term can be used to calculate the effect of splices in top plates of WSP diaphragms where continuous top plates are the designed chord element.

For chord axial forces that are inset from the diaphragm edges, Lawson et al. (2023) provides equations for δ_{flex} and δ_{chord} that use the moment arm distance d between chord forces, instead of full diaphragm width (W) that applies when chords such as spandrel beams frame the edges. Flexural deformations, δ_{flex}, furthermore, depend on the cross-sectional area and modulus of elasticity of the chord. For glulam chords, the cross-sectional area and effective modulus of elasticity of the glulam determine the axial stiffness used for the δ_{flex} calculation. For CLT chords, only the area of laminations with wood fibers aligned parallel with the direction of axial force A_{parallel} and the corresponding modulus of elasticity E for laminations (ANSI/APA 2020) determine the axial stiffness used in the δ_{flex} calculation.

The mechanics-based derivation for the nail slip's contribution to diaphragm deflection δ_{slip} is more accurate when panelization is relatively fine instead of being coarse-compared with the diaphragm size. Designers are cautioned that panel lengths that are larger than half of a simply supported diaphragm span may result in inaccuracies to the nail slip term, and it may be more appropriate to compute the effects of the nail slip based on the actual joint locations following the mechanics of the derivation procedure (Lawson et al. 2023). Another issue for designers to be aware of is that the 2021 SDPWS does not contain prescriptive length-to-width aspect ratio limits for CLT diaphragms as it does for WSP diaphragms. Although the mechanics-based diaphragm deflection derivation theoretically can apply to a wide range of aspect ratios, large-aspect-ratio diaphragms have a disproportionate emphasis on flexural behavior in which the accuracy of chord and chord slip modeling becomes much more important.

Shear deformations of CLT panels contribute to the cumulative δ_{shear} term of diaphragm deflections. US standards typically publish the in-plane shear stiffness of panels using the notation $G_e t_p$ for CLT and $G_v t_v$ for WSP. CLT manufacturers can test and publish in-plane shear stiffness values using test procedures defined in PRG 320.

Several analytical models for effective in-plane shear stiffness of CLT have been developed, based on such testing. G_e is the in-plane, edgewise, shear stiffness of CLT (psi) that depends on layup orientation of orthotropic materials, and t_p is the panel thickness. Flaig and Blaβ (2013) proposed an approach to calculate G_e, which has seen significant application in design (AWC 2021; Spickler et al. 2015). Observing the tests conducted at the Oregon State University, however, Zimmerman and McDonnell (2017) concluded that Flaig and Blaβ's model of in-plane shear stiffness typically underestimates the tested in-plane shear stiffness and often by more than half. Brandner et al. (2017) revised the predictions of G_e, but Zimmerman and McDonnell (2017) found that G_e varies nonlinearly and results in the accuracy of Brandner et al. (2017) to be better at higher shear stresses than at very low shear stresses. Additional research of in-plane stiffness and strength of CLT panels (Nairn 2017; Turesson et al. 2019) has identified several factors that significantly influence in-plane shear stiffness, including board dimensions, the size of gaps, and distribution of cracks. This variability makes estimates of in-plane shear stiffness uncertain, so enveloping previously reported data makes for a reasonable approach to calculating the magnitude of the shear displacement term of CLT diaphragm deflections.

Experimental Validation

Many of the experimental WSP diaphragm tests with deflection results on nonproprietary systems are diaphragms constructed with one nail size and one edge nail spacing throughout, and early research results validated the fundamentals behind Eq. (1) (Tissell and Elliott 2004). The difficulty of conducting experimental research on diaphragm specimens large enough to capture all four deformation components in Eq. (2) hinders the efforts made in the direction of experimental validation, especially considering the difficulty of validating the individual deformation components in isolation and the effects of roofing and flooring overlays. Given the advances in research laboratory capabilities, this would be a welcome area of new research. In an existing rectangular building with a panelized WSP roof diaphragm, Zapata-Kraft et al. (2022) compared the predicted seismic response with the actual response found from strong motion instrumentation and found excellent correlation when refining the stiffness models using the equations and principles discussed herein. Although there are only limited experimental data on large diaphragms that are more consistent with current practices, this paper with its companion (Lawson et al. 2023) provides a mechanics-based approach that improves upon the current approach for blocked WSP diaphragms specified in building code standards.

The use of experimental results from CLT diaphragm tests to validate mechanics-based deflection estimates is an area of ongoing research. Bhardwaj et al. (2021), for example, has offered estimated diaphragm deflections. Other recent tests of full-scale CLT diaphragms (Line et al. 2022a, b) have been conducted to further develop general guidelines for CLT diaphragms in SDPWS. Until further experimental diaphragm deflection research is conducted, the equations presented in this paper provide a rational, mechanics-based approach appropriate for design and analysis.

Conclusions

Today's WSP diaphragms frequently do not match standard assumptions used in the original derivation of the diaphragm deflection model, first developed in the early 1950s. Building upon the generalized standard diaphragm deflection equations derived in the first companion paper (Lawson et al. 2023), a useful diaphragm deflection equation targeted toward current WSP practice is proposed, which addresses variations in nail spacings, panel sizes, and panel orientations.

With the increasing popularity of CLT floor and roof decks, the mechanics-based generalized diaphragm deflection model provides a method to comply with current building code standards, but designers must consider the unique aspects that current CLT construction practices create. The ways of determining appropriate panel

J. Archit. Eng., 2023, 29(3): 04023020

shear stiffnesses, panel-to-panel shear transfer stiffnesses, and active chords and chord splices are quite different from those of past WSP practice. Based on the mechanics of panelized assembly, however, CLT diaphragms share a lot in common with WSP diaphragm behavior, which makes a unified approach possible.

Data Availability Statement

All data, models, and codes generated or used during the study appear in the published article.

Acknowledgments

Funded by U.S. Endowment for Forestry and Communities with matching funds from the USDA Forest Service

Notation

The following symbols are used in this paper:

A = area of a diaphragm chord (in.^{2});
a = exponential behavior variable of the nail slip term e_n in SDPWS Table C4.2.3D;
b = ratio of edge fastener spacings, $S_\perp/S_\parallel$;
E = modulus of elasticity of diaphragm chords (lb$_f$/in.^{2});
e_f = fastener slip along a panel edge;
$e_{f\parallel}$ = fastener slip along a panel edge parallel to the diaphragm load direction based on shear along the diaphragm boundary;
$e_{f\perp}$ = fastener slip along a panel edge perpendicular to the diaphragm load direction based on shear along the diaphragm boundary;
e_n = nail slip measured parallel to the nearest panel edge based on shear along the diaphragm boundary (in.);
G_a = apparent diaphragm shear stiffness (kips/in.);
$G_v t_v$ = panel in-plane, through-the-thickness, shear stiffness (lb$_f$/in. of depth) of WSP panels;
L = length of a diaphragm span, perpendicular to the diaphragm load direction (ft);
$n_\parallel$ = number of slip planes at panel-to-panel connections parallel to the diaphragm load direction;
$n_\perp$ = number of slip planes at panel-to-panel connections perpendicular to the diaphragm load direction;
$P_\parallel$ = panel dimension parallel to the diaphragm load direction;
$P_\perp$ = panel dimension perpendicular to the diaphragm load direction;
$S_\parallel$ = fastener spacing on panel edges parallel to the diaphragm load direction;
$S_\perp$ = fastener spacing on panel edges perpendicular to the diaphragm load direction;
V_f = shear force per fastener;
$V_{f\parallel}$ = shear force per fastener on a panel edge parallel to the diaphragm load direction;
$V_{f\perp}$ = shear force per fastener on a panel edge perpendicular to the diaphragm load direction;
V_n = shear force per nail;
$V_\parallel$ = total shear on a panel edge parallel to the diaphragm load direction;
$V_\perp$ = total shear on a panel edge perpendicular to the diaphragm load direction;
v = induced shear per unit length typically at the diaphragm boundary/support line (lbs/ft);
W = width of the diaphragm, parallel to the diaphragm load direction (ft);
x = distance from the nearest diaphragm support to the location of interest (ft);
Δ_c = diaphragm chord splice slip at the induced unit shear (in.);
δ_{chord} = diaphragm deformation component from the chord slip;
δ_{dia} = diaphragm deformation;
δ_{flex} = diaphragm deformation component from bending;
δ_{shear} = diaphragm deformation component from panel shear deformation;
δ_{slip} = diaphragm deformation component from the panel fastener slip; and
γ = fastener slip stiffness, or slip modulus.

References

ANSI/APA (American National Standards Institute). 2020. *Standard for performance-rated cross-laminated timber*. ANSI/APA PRG 320-2019. Tacoma, WA: APA—The Engineered Wood Association.

ASCE. 2017. "Chapter 7: Analysis procedures and acceptance criteria." In *Seismic evaluation and retrofit of existing buildings*. ASCE/SEI 41-17. Reston, VA: ASCE.

ASCE. 2022. "Chapter 12: Seismic design requirements for building structures." In *Minimum design loads and associated criteria for buildings and other structures*. ASCE/SEI 7-22. Reston, VA: ASCE.

AWC (American Wood Council). 2015. *General dowel equations for calculating lateral connection values*. Technical Rep. 12. Leesburg, VA: AWC.

AWC (American Wood Council). 2021. *Special design provisions for wind and seismic*. Leesburg, VA: AWC.

Bhardwaj, B., W. Pang, D. R. Rammer, M. O. Amini, and S. E. Pryor. 2021. "Experimental performance testing of cantilever cross-laminated timber (CLT) diaphragm under in-plane shear." In *Proc., World Conf. on Timber Engineering*. Santiago, Chile: Centro UC de Innovación de Madera.

Brandner, R., P. Dietsch, J. Dröscher, M. Schulte-Wrede, H. Kreuzinger, and M. Sieder. 2017. "Cross laminated timber (CLT) diaphragms under shear: Test configuration, properties and design." *Constr. Build. Mater.* 147: 312–327. https://doi.org/10.1016/j.conbuildmat.2017.04.153.

BSSC (Building Seismic Safety Council). 2021. *Recommended future issues and research needs—Identified during the development of the 2020 NEHRP recommended seismic provisions for new buildings and other structures*. Washington, DC: National Institute of Building Sciences' Building Seismic Safety Council Provision Update Committee.

CEN (European Committee for Standardization). 2004. *Design of timber structures*. EN 1995-1:2004+A1. Eurocode 5. Brussels, Belgium: CEN.

Cobeen, K. E., J. D. Dolan, D. Thompson, and J. W. van de Lindt. 2014. *Seismic design of wood light-frame structural diaphragm systems: A guide for practicing engineers*. Applied Technology Council. Gaithersburg, MD: NIST.

Countryman, D. 1952. *Lateral tests on plywood sheathed diaphragms*. Tacoma, WA: Douglas Fir Plywood Association.

CSA (Canadian Standard Association). 2019. *Engineering design in wood*. CSA 086-14 (Reaffirmed 2019). Toronto: CSA.

Dolan, J. D., D. M. Carradine, J. W. Bott, and W. S. Easterling. 2003. *Design methodology of diaphragms*. Richmond, CA: Consortium of Universities for Research in Earthquake Engineering.

FEMA. 2021. *Seismic design of rigid wall-flexible diaphragm buildings: An alternative procedure*. 2nd ed. FEMA P-1026. Washington, DC: FEMA.

Flaig, M., and H. J. Blaβ. 2013. "Shear strength and shear stiffness of CLT-beams loaded in plane." In Proc., *CIB-W18 Meeting 46*. Vancouver, BC: International Council for Research and Innovation in Building and Construction.

Foster, R. M., T. Reynolds, and M. Ramage. 2016. "Proposal for defining a tall timber building." *J. Struct. Eng.* 142 (12): 02516001. https://doi.org/10.1061/(ASCE)ST.1943-541X.0001615.

Gagnon, S., T. Bilek, L. Podesto, and P. Crespell. 2013. "Introduction to cross-laminated timber." In *CLT handbook: Cross-laminated timber, U.S. edition*, edited by E. Karacabeyli and B. Douglas. Point-Claire, Quebec: United States Department of Agriculture (USDA)/U.S. Forest Service/Forest Products Laboratory and Binational Softwood Lumber Council (BSLC).

ICC (International Code Council). 2021. *International building code*. Country Club Hills, IL: ICC.

Laguarda-Mallo, M. F., and O. Espinoza. 2018. "Awareness, perceptions and willingness to adopt CLT by US engineering firms." *BioProducts Bus.* 3 (1): 1–14.

Lawson, J. W. 2012. *Seismic design of timber panelized roof structures: 2012 International Building Code (IBC) edition*. Washington, DC: Woodworks.

Lawson, J. W. 2018. "Improving the accuracy of wood diaphragm deflection estimates." *Wood Des. Focus* 28 (2): 40–46.

Lawson, J. W. 2019. "Improving the accuracy of wood diaphragm deflection computations and its impact on ASCE 41 pseudo-lateral force estimates." In *Proc., Structural Engineers Association of California Convention*. Squaw Valley, CA: Curran Associates.

Lawson, J., and M. Koliou. 2020. "Evaluating second order effects in rigid wall-flexible roof diaphragm buildings." *Earthquake Spectra* 36 (4): 1864–1885. https://doi.org/10.1177/8755293020919420.

Lawson, J., S. Breneman, and M. Lo Ricco. 2023. "Wood diaphragm deflections. Part I: Generalizing standard equations using mechanics-based derivations for panel construction." *J. Archit. Eng*. https://doi.org/10.1061/JAEIED.AEENG-1573.

Line, P., S. Nyseth, and N. Waltz. 2022a. "Full-scale cross-laminated timber diaphragm evaluation. I: Design and full-scale diaphragm testing." *J. Struct. Eng.* 148 (5): 04022037. https://doi.org/10.1061/(ASCE)ST.1943-541X.0003308.

Line, P., S. Nyseth, and N. Waltz. 2022b. "Full-scale cross-laminated timber diaphragm evaluation. II: CLT diaphragm connection tests." *J. Struct. Eng.* 148 (5): 04022038. https://doi.org/10.1061/(ASCE)ST.1943-541X.0003309.

Nairn, J. A. 2017. "Cross laminated timber properties including effects of non-glued edges and additional cracks." *Eur. J. Wood Prod.* 75 (6): 973–983. https://doi.org/10.1007/s00107-017-1202-y.

NZS (New Zealand Standards). 1993. *Timber structures standard*. NZS 3603:1993. Wellington, New Zealand: NZS.

Pang, W., S. Pant, C. Ni, and J. Lawson. 2014. "Examining the applicability of design methods for large panelized all-wood roof diaphragms under seismic loading." In Proc., *10th US National Conf. on Earthquake Engineering*. Oakland, CA: Earthquake Engineering Research Institute.

SEAOC (Structural Engineers Association of California). 2019. *2018 IBC SEAOC structural/seismic design manual, volume 2, example 2*. Sacramento, CA: SEAOC.

Skaggs, T. D., and Z. A. Martin. 2004. "Estimating wood structural panel diaphragm and shear wall deflection." *Pract. Period. Struct. Des. Constr.* 9 (3): 136–141. https://doi.org/10.1061/(ASCE)1084-0680(2004)9:3(136).

Spickler, K., M. Closen, P. Line, and M. Pohil. 2015. "Cross laminated timber: horizontal diaphragm design example." *Penticton, BC: Structurlam. Revision 10*. Accessed January 23, 2023. www.structurlam.com/resources/manufacturing-standards/.

Sullivan, K., T. H. Miller, and R. Gupta. 2018. "Behavior of cross-laminated timber diaphragm connections with self-tapping screws." *Eng. Struct.* 168: 505–524. https://doi.org/10.1016/j.engstruct.2018.04.094.

Taylor, B., A. R. Barbosa, and A. Sinha. 2020. "Cyclic performance of in-plane shear cross-laminated timber panel-to-panel surface spline connections." *Eng. Struct.* 218: 110726. https://doi.org/10.1016/j.engstruct.2020.110726.

Taylor, B., A. R. Barbosa, and A. Sinha. 2021. "In-plane shear cyclic performance of spline cross-laminated timber-concrete composite diaphragms." *J. Struct. Eng.* 147 (10): 04021148. https://doi.org/10.1061/(ASCE)ST.1943-541X.0003127.

Tissell, J. R., and J. R. Elliott. 2004. *Plywood diaphragms*. Tacoma, WA: APA—The Engineered Wood Association.

Turesson, J., S. Berg, and M. Ekevad. 2019. "Impact of board width on in-plane shear stiffness of cross-laminated timber." *Eng. Struct.* 196: 109249. https://doi.org/10.1016/j.engstruct.2019.05.090.

Zapata-Kraft, C., J. Lawson, and P. Laursen. 2022. "Estimating periods of wood structural panel diaphragms." In *Proc., 12th U.S. National Conf. on Earthquake Engineering*. Oakland, CA: Earthquake Engineering Research Institute.

Zimmerman, R. B., and E. McDonnell. 2017. "Framework—A tall re-centering mass timber building in the United States." In *Proc., Joint 2017 New Zealand Society for Earthquake Engineering Annual Conf. and the Anti-Seismic Systems International Society's 15th World Conf.* Wellington, New Zealand: New Zealand Society for Earthquake Engineering.